Fundamental Concept of Designing Tunnel Supports in Consideration of Elasto-plastic and Strain Softening Behavior of Rock

By

Chikaosa TANIMOTO* and Shojiro HATA*

(Received June 2, 1980)

Abstract

The rapid increase in tunnelling projects requires better design methods which can deal with the post-peak behavior of soft rock subjected to heavy loads. The analytical solution for strain softening behavior of rock around a circular opening is derived from the strain energy theorem employing Coulomb's yield criterion. Using a simplified stress-strain relation, it is possible to obtain uniquely the magnitudes of stress, strain and displacement in elastic, softening and flow states by using only 10 input data: radius of a circular opening, hydro-static initial stress field, equivalent inner pressure to reaction of supports, elastic modulus, Poisson's ratio, negative gradient of deformation coefficient, and peak and residual strengths (uniaxial compressive strengths and angles of internal friction).

Case studies conclude that a small increase of inner pressure has a large influence on the width of the plastic zone in rock which has induced softening. They also show that there is a big difference between a strain softening model and a conventional bi-linear elasto-plastic model, for the case of rock having a low competence factor. Herein, the authors discussed a procedure to design a support system, including rockbolts and shotcrete, by replacing the supports by an inner pressure acting on the surface of the tunnel wall.

1. Introduction

In most cases of tunnel driving through rock, the fundamental requirement is how to advance the mining face so as to make the original state of the ground as undisturbed as possible. It can be pointed out (with the exception of seriously creeping ground) that the most predominant deformation occurs in the vicinity of the advancing face. It is subjected to a positional (geometrical) condition, judging from experience and the observations of convergence surveys which showed that the increase of convergence was almost negligible when (the advance of) the face stopped. The surveys also showed

* Department of Civil Engineering

that the time dependency of deformation depended on the progressive failure of rock, caused by having allowed too much displacement near the opening. This means that the face plays an important role as a temporary support. The rock mass near the face is stabilized by the 'half-dome action' in the profile and the 'ring action' in the cross section. When advancing the face, it is required to place artificial supports to substitute for the half-dome action within a span length from the face, in the driving direction, so as to mobilize the bearing capacity of the rock mass as fully as possible.

The so-called New Austrian Tunnelling Method (NATM), where rock-bolting and shotcrete lining are applied, is the latest and most feasible tunnelling method for this purpose, especially from the practical point of view. Such supports as rockbolts, shotcrete lining and steel arch ribs are placed tightly near the face, and are subjected to a three dimensional stress field. The main subject discussed in the following sections is how to design a support system, considering the half-dome action given by the face itself, and the elastic/elasto-plastic behavior of the rock mass. From the point of view that the effects of systematic supports are 'mobilizing confining stress' and 'decreasing shear stress', a procedure to design supports can be proposed by replacing the effects of the supports by the inner pressure acting on the surface of the tunnel wall.

The competence factor (C_f) is defined as the ratio of unconfined compressive strength (q_u) to overburden pressure (i.e. $\rho \cdot h$, the product of density ρ and depth h), $q_u/\rho \cdot h$.[1] Based on the observed behavior at more than 50 tunnelling sites in Japan, Nakano points out the relation between the rock pressure and the competence factor as follows[2]:

$C_f > 10$ for slight or no rock pressure,
$4 < C_f \leqq 10$ for loosening rock pressure,
$2 < C_f \leqq 4$ for light~large squeezing rock pressure,
$C_f \leqq 2$ for heavy~very heavy squeezing-swelling rock pressure

There has been no discussion in detail for the case of $C_f \leqq 2$.

In this range, the following discussion will give more detailed analysis and information for a practical design of tunnels.

2. Basic Idea of Tunnelling

Consider a circular opening in an isotropic stress field p_0, as shown in Fig. 1.

In this figure, the state of (A), on the left hand side, is the most conventional model. However, when we discuss supports in tunnelling, it is important to consider the timing of the setting supports and the stress changes caused by the advance of the mining face. The state of (B), in the middle, shows the initial state, being subjected to primary stress (p_0). The state of (C), on the right hand side, shows the stress concentrations around

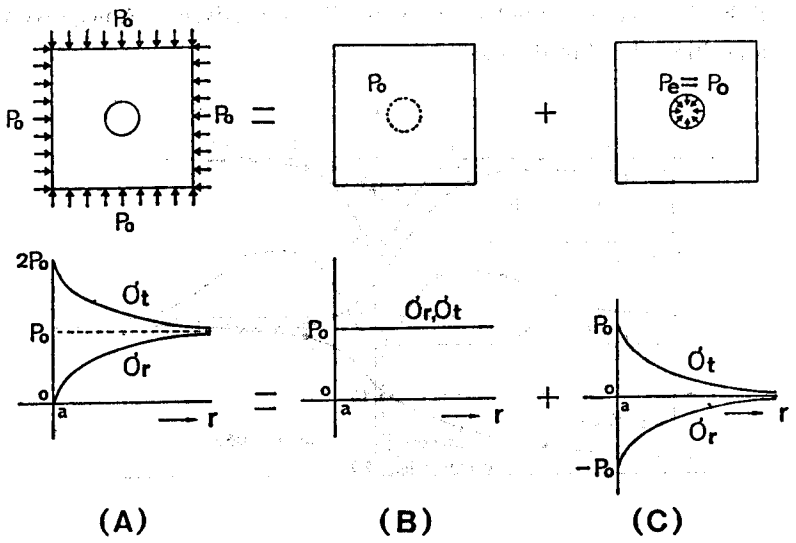

Fig. 1 Stress around a circular opening

a circular opening caused by the extraction force acting on the wall of the opening, without the primary stress.

State (A) is obtained by superposing state (C) on state (B). In tunnelling, state (B) exists before excavation.

When we pay attention to the change of the extraction force p_e, which is equal to p_0 in case of no support and is sometimes called 'excavation force', we can explain the basic idea of tunnelling very easily. Fig. 2 shows the stress state near the face.

By the result of a simple FEM computation using an axi-symmetric model, we obtain the stress-changes of σ_r, σ_t, σ_z and τ_{rz} as shown in Fig. 3. The notations 'a', 'r' and 'd' are the radius of a circular opening, the distance from the center in the cross

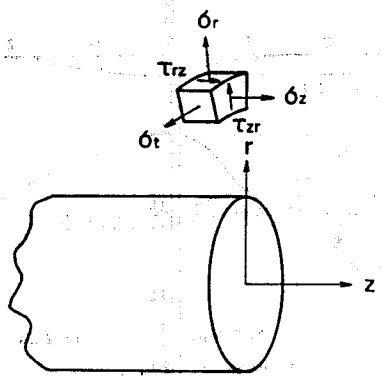

Fig. 2 Stress state near the face

section, and the distance from the face in the profile, respectively. A negative value of 'd' means a position ahead of the face.

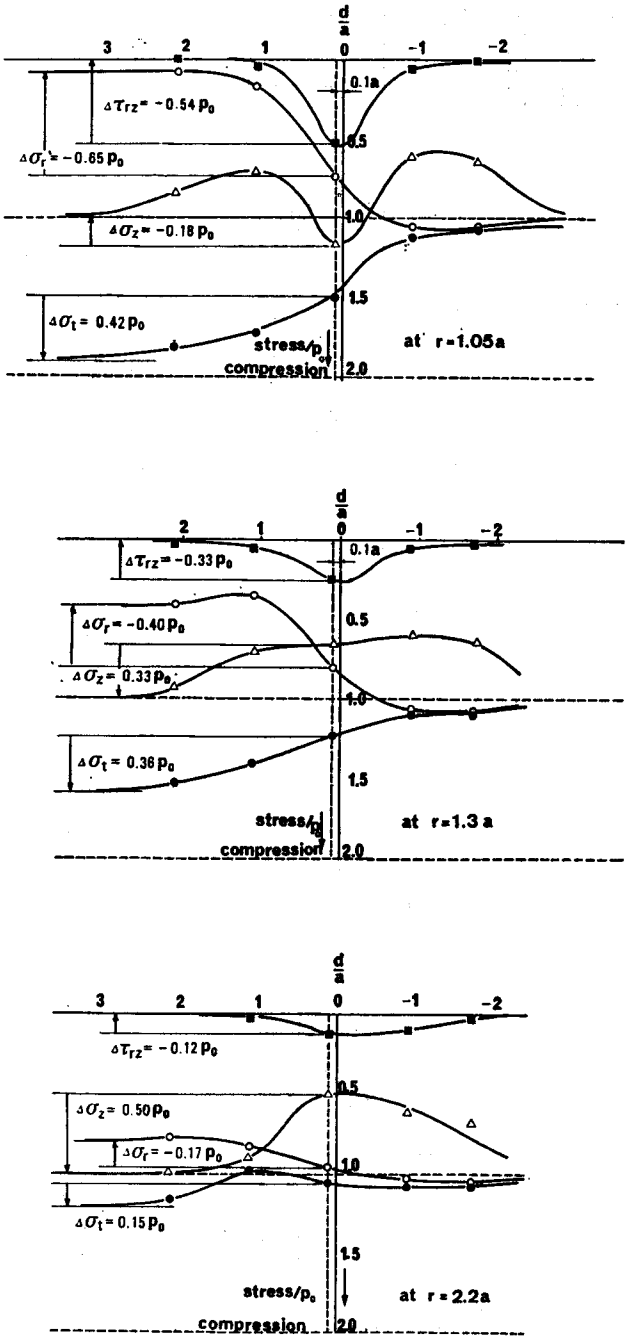

Fig. 3 Stress changes caused by the advance of the face

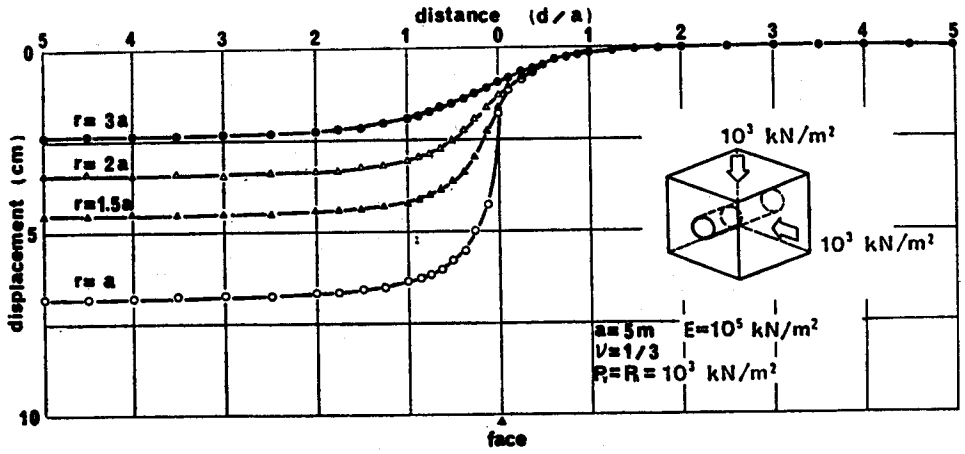

(a) A circular opening

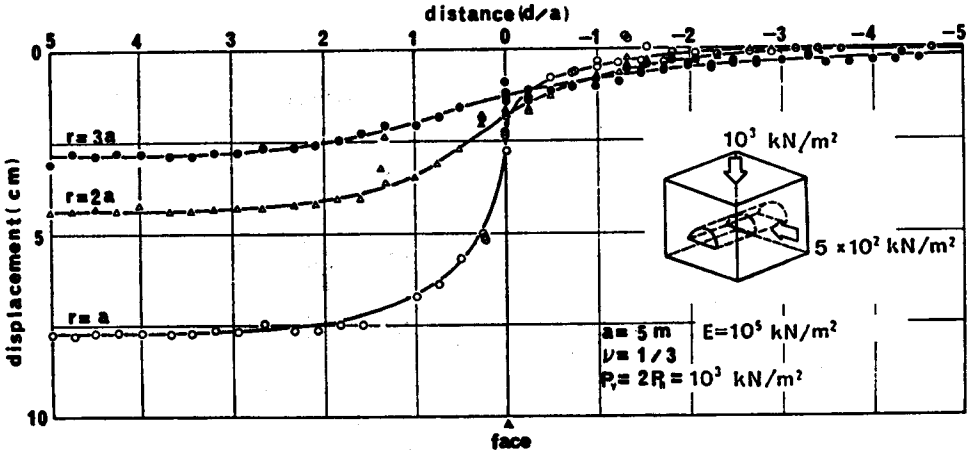

(b) A semi-circular opening

Fig. 4 Theoretical displacement curves for an elastic body

To speak of the case at $r=1.05\,a$ near the wall, the radial normal stress σ_r varies from p_0 to $2p_0$, and the normal stress σ_z and the shear stress τ_{rz} vary only near the face. Among these stresses, σ_r especially corresponds to the change of the wall displacement, that is, the convergence curve.

The displacement curves in Fig. 4 show a theoretical curve of displacement for an elastic body. The displacement varies within the range of $d/a=-2$ or -3 and $d/a=2$ or 3. Fig. 5 shows the displacement curves obtained by field measurements which were carried out in the Kameura and Seikan Tunnels.[3,4] Fig. 6 shows the change of the

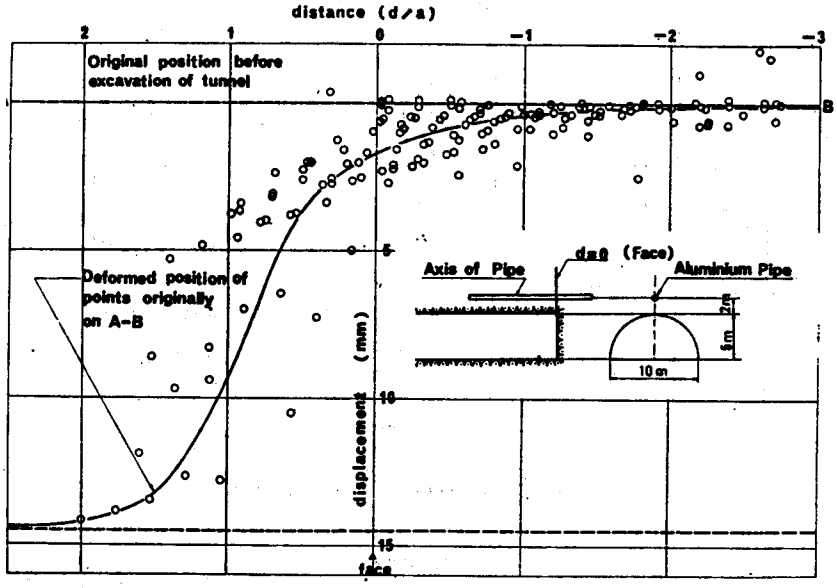

(a) Kameura Tunnel through shale-sandstone [3]

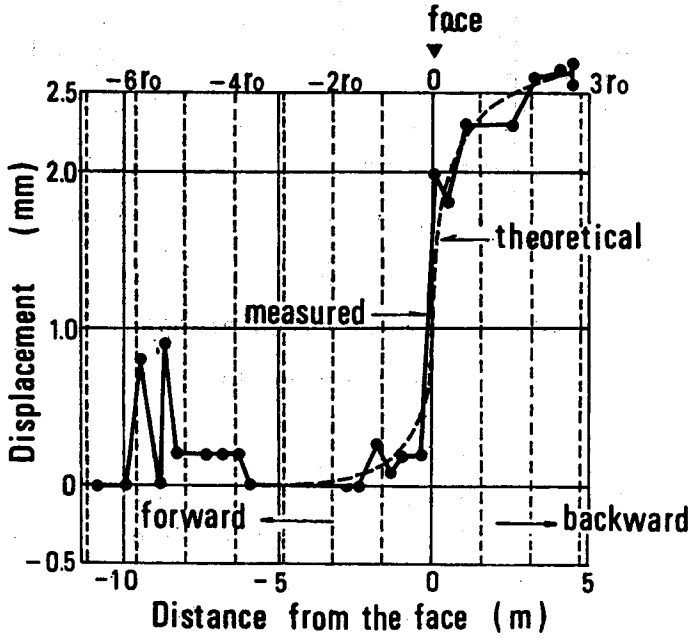

(b) Seikan Tunnel through andesite-tuff [4]

Fig. 5 Measured displacement curves during construction

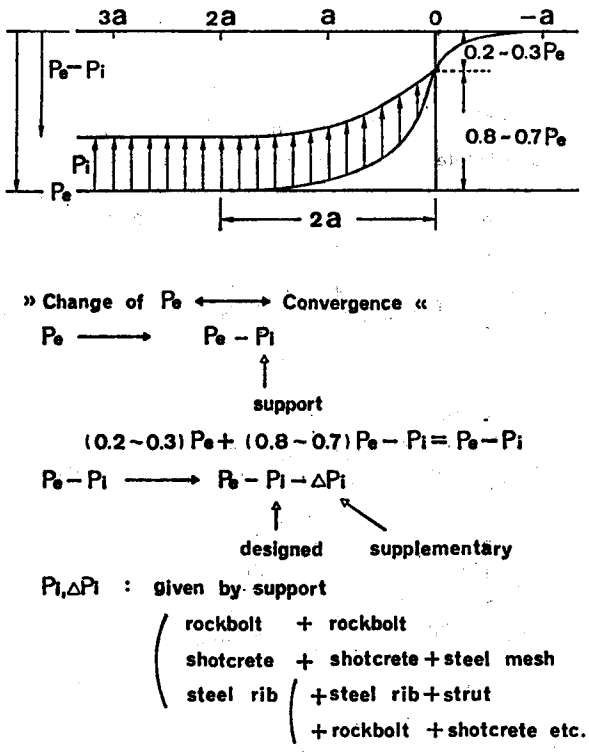

Fig. 6 Superposed forces around an opening induced by exacavation

extraction force mentioned already. Without support, p_e varies from zero to p_0. The increase of p_0 has a one to one correspondence to the decrease of σ_r. Consequently, a convergence survey means monitoring the change of σ_r or the extraction force p_e as well as the displacement of the wall. When it is found that the bearing capacity of the ground is insufficient without any artificial supports in the final state, it is required to introduce an inner pressure p_i, mobilized by the reaction of the supports, and only pre-stressing rockbolts can give an active p_i.

By considering this "p_i" as a main parameter, we can calculate the width of the plastic zone, the displacement of the wall and the plastic strain near the wall, and can design the support system.

3. Design of Pre-stressed Type Rockbolt Support

By assuming a circular tunnel driven through ground being subjected to an isotropic stress field p_0, it is possible to discuss the behavior of the ground near opening. Fig. 7 shows the change of three dimensional stresses at $r=1.05a$ (near wall), $1.3a$ and $2.2a$, and we can image how Mohr's circle varies from the initial state to the final one. Also,

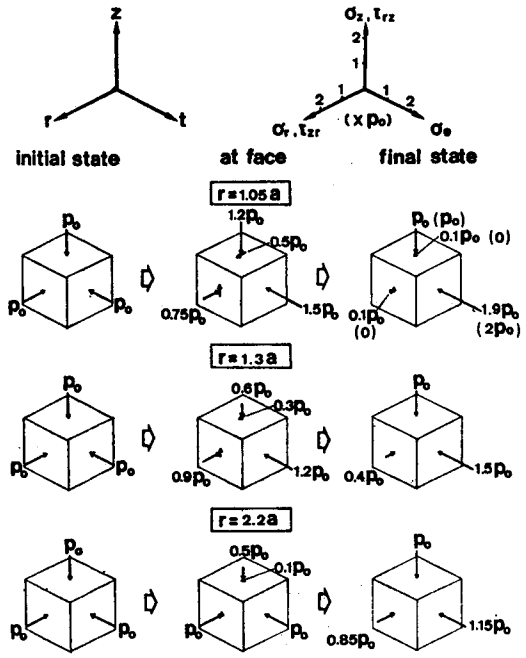

Fig. 7 Three dimensional state of stresses associated with the advance of the face

Fig. 8 shows the state of principal stress directions and the displacement of free surface. When fully bonded systematic rockbolts are placed near the face (d=0.1 a, 50 cm behind

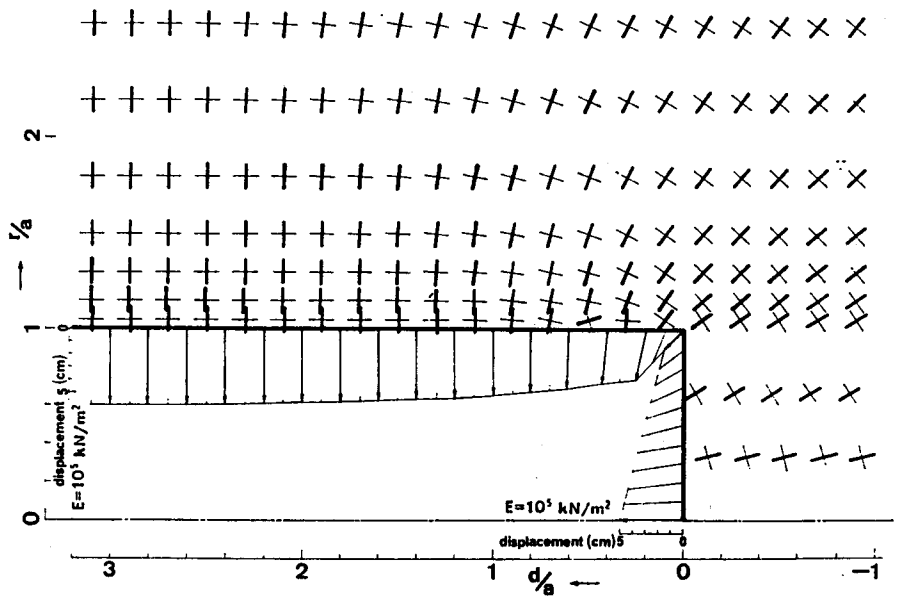

Fig. 8 Directions of principal stresses and displacement of a free surface

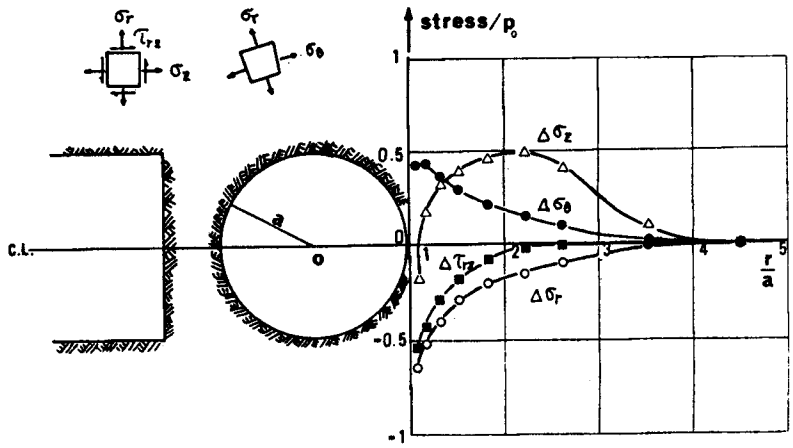

Fig. 9 Stress increments acting on a fully bonded rockbolt

of the face in the case of a conventional two-lane motorway tunnel), and the ground behaves in the manner of an elastic body, each rockbolt may finally be subjected to the stress increments as shown in Fig. 9. The difference between systematic bolting placed only at a single cross section and placed serially at the interval of 1 m in the profile can be seen in Fig. 10.

Next, before discussing designing the rockbolt supports, let touch on the distribution of the plastic zone around an opening. Fig. 11 shows the plastic zone obtained by a parametric analysis based on Drucker's plasticity criterion. The radius of an opening is 5 m and the notation C and ϕ mean the cohesion and the angle of internal friction, respectively. From Fig. 8 and Fig. 11 we can presume the effect of spiling rockbolts

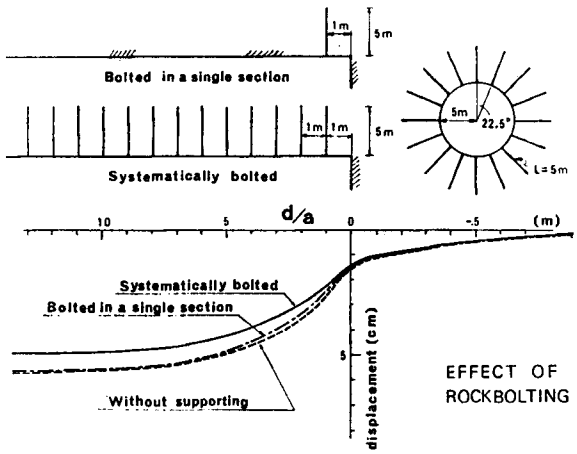

Fig. 10 Decrease of displacement by systematic rockbolts in an elastic body (Elastic constant for the ground $E=10^5$ kN/m²)

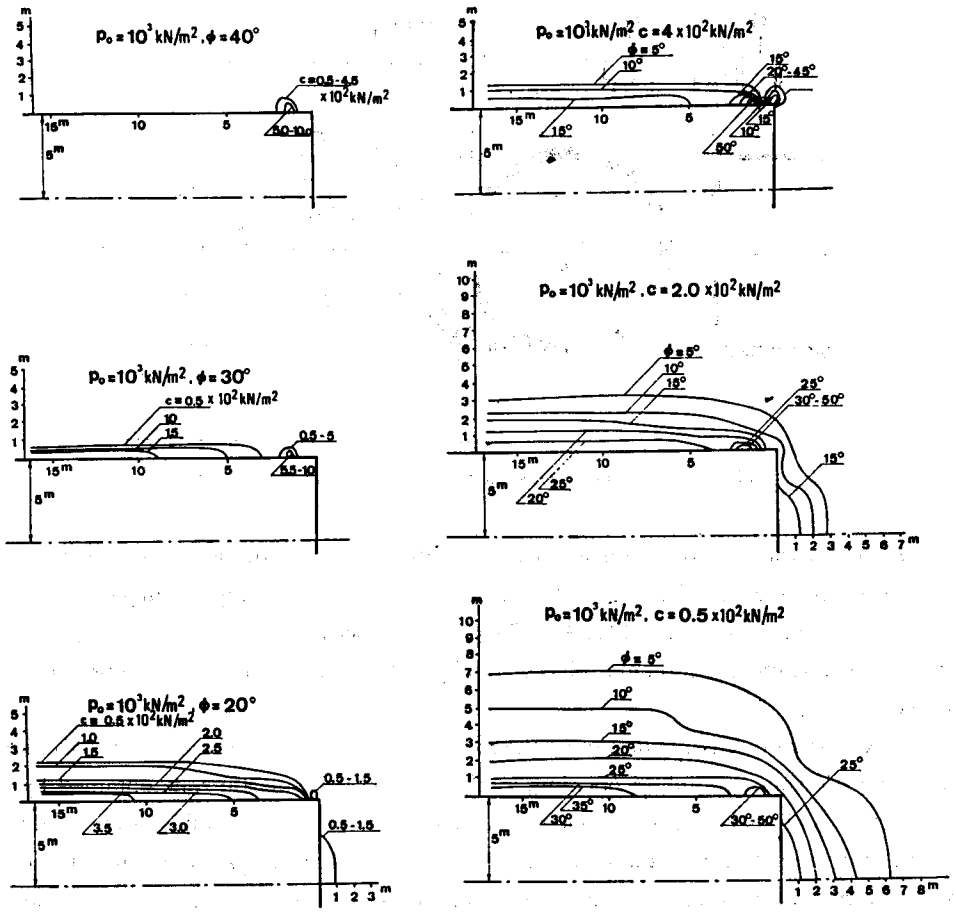

Fig. 11 Distribution of plastic zone

for the pre-reinforcement and bolting on the mining face. Under the condition of $p_0=10^3$ kN/m^2, the relationships in the plastic zones, C and ϕ, are shown by Fig. 12.

If the ground deforms as a continum in the elastic range, no support will be required. But, as a matter of course, it is confirmed that the plastic behavior of the ground should be considered in designing the support.

Then, let us proceed in our discussion on designing supports by using an elasto-plactic (strictly speaking, elastic-perfectly plastic) model, as shown in Fig. 13.

When Coulomb's yield criterion is employed, the width of the plastic zone W_1, the displacement of the wall U_w and the mean plastic strain ε_p, defined by $(\varepsilon_{t,\,\text{plastic}}-\varepsilon_{r,\,\text{plastic}})$, can be expressed in the forms of the following equations, by giving figures to the radius of a circular opening a, elastic constant E, Poisson's ratio ν, unconfined compressive strength q_u, angle of internal friction ϕ, hydrostatic initial stress field p_0 and support-reaction (bearing capacity of supports) p_i.

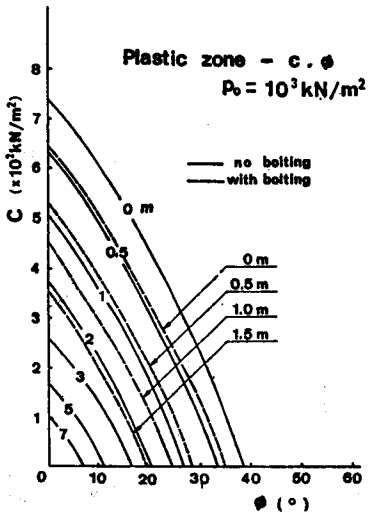

Fig. 12 C, ϕ and plastic zone

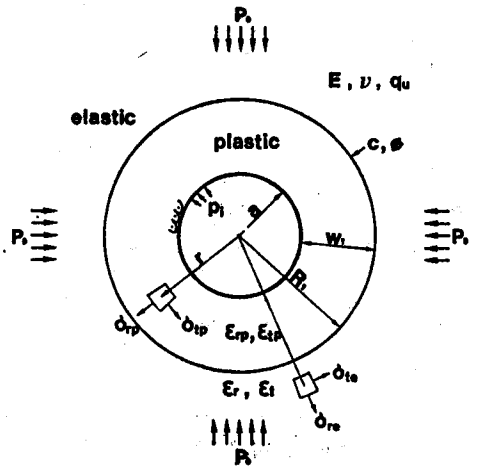

Fig. 13 Analytical model for elasto-plastic behavior

$$W_1=a\left[\frac{2\{p_0(\zeta-1)+q_u\}}{(1+\zeta)\{(\zeta-1)p_i+q_u\}}\right]^{\frac{1}{\zeta-1}}-a \tag{1}$$

$$U_w=\frac{1}{2\mu}\left\{p_0-\frac{2p_0-q_u}{1+\zeta}\right\}\cdot\frac{R_1^2}{a} \tag{2}$$

$$\epsilon_\theta=\frac{p_0(\zeta-1)+q_u}{\mu(1+\zeta)}\cdot\left\{\frac{R_1}{a}-\frac{1}{\zeta}\cdot\frac{R_1^\zeta-a^\zeta}{R_1^{\zeta-1}(R_1-a)}\right\} \tag{3}$$

where

$$\zeta=\frac{1+\sin\phi}{1-\sin\phi},\qquad \mu=\frac{E}{2(1+\nu)}$$

Being based on the results of laboratory tests, let us assume the allowable plastic strain to be 2.5%. This is the first step in the design process.

Fig. 14 (a), (b) and (c) have the same parameter p_i with respect to abscissa under the same conidition of $p_0=3\times10^3$ kN/m², $E=2\times10^5$ kN/m². When we pick the case of $\phi=20°$ (curve ⑤), we can read the value of p_i corresponding to $\varepsilon_\theta=2.5\%$ in the figure on the right hand side, namely $p_i=200$ kN/m². In the case of applying p_i of 200 kN/m², we can read the displacement of the wall, namely, $U_w=0.20$ m. Therefore, 70–80% means the quantities of displacement which occur from the position of the face ($d/a=0$) as mentioned before. For the observational construction, the limit of allowable convergence should be 30 cm. When $p_i=2.0\times10^2$ kN/m², the width of the plastic zone becomes 6.5 m. Fig. 15 shows the bearing capacity of fully bonded rockbolts 10 m long, which is determined from a value of 1.5 times W_p (width of plastic zone). Also from Fig. 15, it is concluded that 32 bolts of 25 mm dia. are required to be set (circumferentially) radially per 1 m shift, although the interaction between pre-stressed rockbolts and the ground has not yet been described clearly.

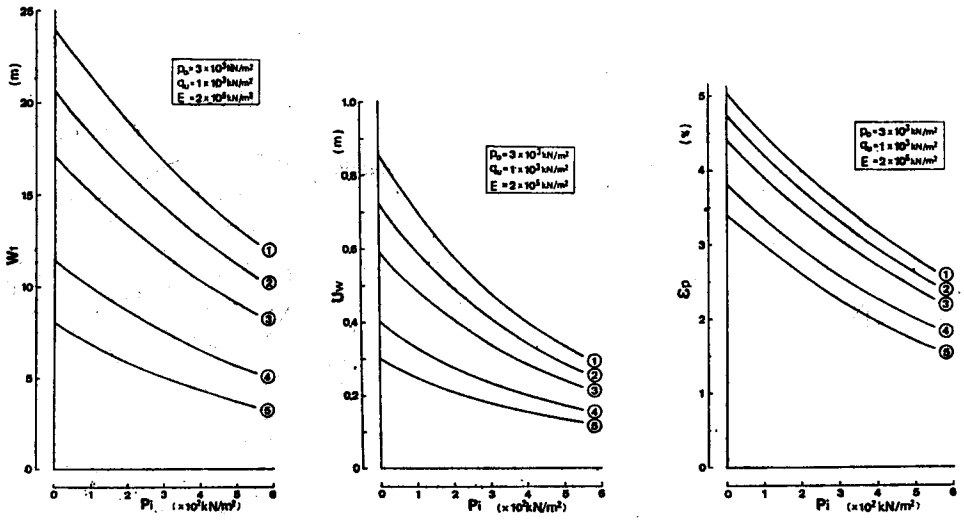

curve	ø (degree)
①	6.5
②	8
③	10
④	15
⑤	20

Fig. 14 Plastic zone, displacement of wall and plastic strain around an opening (p_0=3000 kN/m², q_u=1000 kN/m², E=2×10⁵ kN/m²)

4. Strain Softening Behavior

Through field measurements and observations in the Nabetachiyama Tunnel[5)~7)], we found that the elasto-plastic model could not simulate the actual deformation of the ground very well, and that a consideration of the strain softening behavior was required.

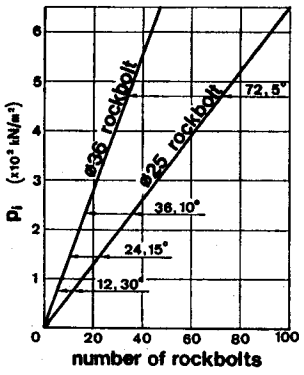

Fig. 15 Bearing capacity of systematic rockbolt supports

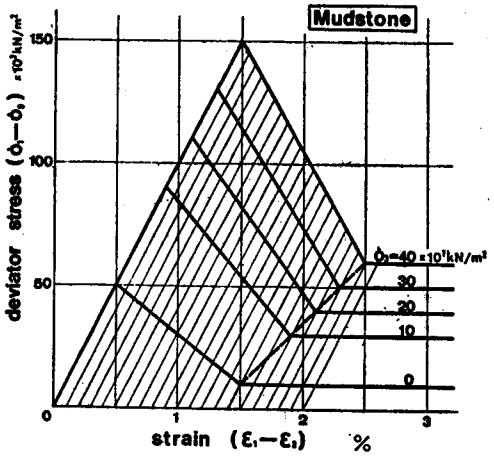

Fig. 16 Schematic stress-strain curves of Nabetachiyama Mudstone

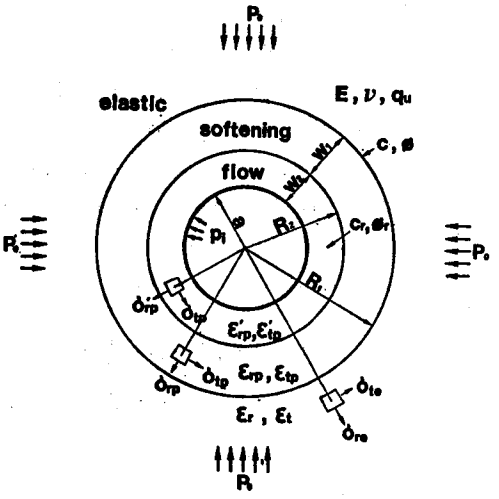

Fig. 17 An idealized strain softening model

From the results obtained by many triaxial tests, we tried to determine schematic stress-strain curves for the Neogene mudstone sampled from the sites of the Nabetachiyama Tunnel, as shown in Fig. 16. As the Neogene formation contained numerous microscopic fissures due to multiple foldings, it was very dificult to get satisfactory specimens having the specified shape and dimension, even in the case of $q_u=3\sim5\times10^3$ kN/m².

Regarding such ground showing typical strain softening behavior, we can assume the idealized model shown in Fig. 17. The width of the plastic zone (W_p) is the sum of the softening zone (W_1) and the flow zone (W_2). The fundamental equations, which express the strain softening behavior, can be derived from strain energy theorems. That is, assume the relationship between the axial stress and the axial strain as shown by the three segmented straight lines in Fig. 18. Then, the rock specimen behaves in the manner of an elastic body along the straight path through Points O, A and B. Then, it takes a softening path to a certain stress level, and thereafter it causes flow at a constant stress level. By simplifying the stress-strain relations in such a way, the

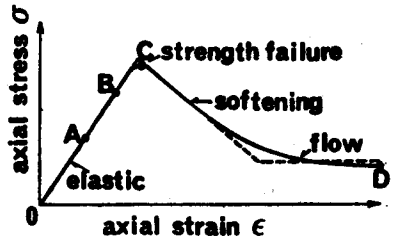

Fig. 18 Stress-strain relation for strain softening

following fact can be confirmed with respect to the product $\sigma\cdot\varepsilon$ of stress σ and strain ε. Namely, in the region exhibiting the elastic behavior, '$\sigma\cdot\varepsilon$' can be expressed in the form of a quadratic function of 'ε'. The increasing rate of $\sigma\cdot\varepsilon$ to ε becomes maximum at Point C, and thenceforth follows the curve in a concave parobolic form. Finally, when flow is caused, $\sigma\cdot\varepsilon$ increases at a constant gradient.[8)]

If it is accepted that the strain continues to increase the total strain energy (W) given to the specimen which shows softening can be expressed in the following form of expansion, in terms of the second degree regarding strain components ε_t and ε_r.

$$W=a+b\varepsilon_t+c\cdot\varepsilon_r+\frac{1}{2}d\varepsilon_t^2+e\cdot\varepsilon_t\cdot\varepsilon_r+\frac{1}{2}f\varepsilon_r^2 \tag{4}$$

where a, b, c, d, e and f are constants.

This strain energy W should agree with the elastic strain energy. According to the definition,

$$\left.\begin{aligned}\sigma_t&=b+d\cdot\varepsilon_t+e\cdot\varepsilon_r\\ \sigma_r&=c+e\cdot\varepsilon_t+f\cdot\varepsilon_r\end{aligned}\right\} \tag{5}$$

Eq. (5) can be rewritetn in the following form.

$$\left.\begin{aligned}\sigma_t&=\left(b-\frac{ec}{f}\right)+\frac{e}{f}\sigma_r+\left(d-\frac{e^2}{f}\right)\varepsilon_t\\ \sigma_t&=\left(b-\frac{dc}{e}\right)+\frac{d}{e}\sigma_t+\left(e-\frac{df}{e}\right)\varepsilon_t\end{aligned}\right\} \tag{6}$$

In a simpler form,

$$\left.\begin{aligned}\sigma_t&=k_1+k_2\sigma_r+k_3\varepsilon_t\\ \sigma_t&=k_4+k_5\sigma_r+k_6\varepsilon_t\end{aligned}\right\} \tag{7}$$

where,

$$\left.\begin{aligned}&k_1=b-\frac{ec}{f},\qquad k_2=\frac{e}{f},\qquad k_3=d-\frac{e^2}{f},\\ &k_4=b-\frac{dc}{e},\qquad k_5=\frac{d}{e},\qquad k_6=e-\frac{df}{e}\end{aligned}\right\} \tag{8}$$

also,

$$k_2\cdot k_6+k_3=0 \tag{9}$$

On the other hand, the elastic strain at the yield point is

$$\left.\begin{aligned}E\cdot\varepsilon_t&=(1-\nu^2)\sigma_t-\nu(1+\nu)\sigma_r\\ E\cdot\varepsilon_r&=-\nu(1+\nu)\sigma_t+(1-\nu^2)\sigma_r\end{aligned}\right\} \tag{10}$$

At the yield point, the stresses and strains given by Eq. (10) agree with those given by Eq. (7).

Here, the Mohr-Coulomb yield criteria is given by the following equation.

$$\sigma_t = q_u + q \cdot \sigma_r \tag{11}$$

where q_u is the unconfined compressive strength, and q is given by

$$q = \tan^2\left(\frac{\pi}{4} + \frac{\phi}{2}\right) \tag{12}$$

where ϕ: angle of internal friction

By substituting Eq. (10) and (11) for Eq. (7), we obtain

$$k_1 - q_u + \frac{k_3}{E}(1-\nu^2)q_u + \left[k_2 - q + \frac{k_3}{E}\{(1-\nu)q-\nu\}(1+\nu)\right]\sigma_r = 0$$

$$k_4 - q_u + \frac{k_6}{E}\nu(1+\nu)q_u + \left[k_5 - q - \frac{k_6}{E}\{\nu q-(1-\nu)\}(1+\nu)\right]\sigma_r = 0$$

As these equations should be valid for any σ_r, the following four equations are obtained for the coefficients $k_1, k_2, \cdots, k_6$:

$$\left.\begin{aligned} &k_1 - q_u + \frac{k_3}{E}(1-\nu^2)q_u = 0 \\ &k_4 - q_u + \frac{k_5}{E}(1+\nu)\nu q_u = 0 \\ &k_2 - q + \frac{k_3}{E}\{(1-\nu)q-\nu\}(1+\nu) = 0 \\ &k_5 - q - \frac{k_3}{E}\{\nu q-(1-\nu)\}(1+\nu) = 0 \end{aligned}\right\} \tag{13}$$

By the assumption that the relation between σ_t and ε_t is shown by the straight line with the negative gradient $(-\omega)$ under constant σ_r, k_3 becomes $-\omega$.

$$k_3 = -\omega \tag{14}$$

ω has the same dimension as the elastic constant E.

By solving Eq. (9), Eq. (13) and Eq. (14) simultaneously, $k_1, k_2, \cdots, k_6$ are obtained in the form of the following equations.

$$\left.\begin{aligned} &k_1 = \left\{1 + \frac{\omega}{E}(1-\nu^2)\right\}q_u \qquad k_2 = q + \frac{\omega}{E}\{(1-\nu)q-\nu\}(1+\nu) = \frac{\omega}{k_6} \\ &k_3 = -\omega \qquad\qquad\qquad\qquad k_4 = \left\{1 + \frac{k_6}{E}(1+\nu)\nu\right\}q_u \\ &k_5 = q + \frac{k_6}{E}\{\nu q-(1-\nu)\}(1+\nu) \qquad k_6 = \frac{\omega}{k_2} \end{aligned}\right\} \tag{15}$$

Consequently, the stress-strain relation in the softening state can be expressed uniquely by the parameters of the elastic constants of E and ν, the yielding constants of q_u and ϕ, and the negative gradient ω. This relation can be applied until the flow begins to occur. The condition of the flow is given by

$$\sigma_t = q_u' + q' \cdot \sigma_r \tag{16}$$

where

$$\sigma_t > \sigma_r, \qquad q' = \tan^2\left(\frac{\pi}{4}+\frac{\phi'}{2}\right) \qquad \text{and}$$

q_u' and ϕ' are the unconfined compressive strength and angle of the internal friction at the residual state, respectively.

The rock in the softening state has the following relation:

$$q_u' + q' \cdot \sigma_r < \sigma_t \leqq q_u + q \cdot \sigma_r \tag{17}$$

Being based on these assumptions, the fundamental equations, which express the elastic-softening behavior and the elastic-softening-flow behavior, can be obtained by the derivation mentioned in reference[8]. In this paper, only the final equations modified for convenient usage are shown.

5. Analytical Solution for Strain Softening Behavior

Input data for calculation or computation are as follows:

- a: radius of a circular opening,
- E: Young's Modulus,
- ν: Poisson's ratio,
- q_u: unconfined compressive strength,
- ϕ: angle of internal friction,
- ω: negative slope of deformation coefficient for softening zone,
- p_0: hydrostatic initial stress,
- p_i: inner pressure acting on the wall of an opening (=reaction of supports),
- q_u': unconfined compressive strength at redsiual state,
- ϕ': angle of internal friction at residual state

Output data are:

- R_1: radius of 'elastic-softening' boundary,
- R_2: radius of 'softening-flow' boundary,
- S_1: ratio of R_1 to R_2 $(=R_1/R_2)$,
- S_2: ratio of R_2 to a $(=R_2/a)$,
- S_3: ratio of R_1 to a $(=R_1/a)$,
- ε_t^*, ε_r^*: strains on the wall in tangential and radial directions respectively,
- σ_t^*, σ_r^*: stresses on the wall in tangential and radial directions,
- U^*: displacement of the wall in the radial direction

Computation procedure is as follows:

There are two cases: the case of induced softening and flow, and the case of induced softening only.

PROCEDURE

Case of induced 'softening and flow'

(1) INPUT DATA:

$$a,\ E,\ \nu,\ q_u,\ \phi,\ \omega,\ p_0,\ p_i,\ q_u',\ \phi'$$

(2) Solve the following equation. (S_1: unknown)

$$A_1 S_1^{-2} - A_2 S_1^{n_2-1} + A_3 S_1^{n_1-1} = 0 \rightarrow S_1 \tag{18}$$

where

$$S_1 = R_1/R_2$$
$$A_1 = (b - d\gamma - e\gamma - q_u' - q'c + q'e\gamma + qf\gamma)(e^2 - df)(n_1 - n_2)$$
$$A_2 = (d + en_1 - q'e - q'fn_1)[\{b - d\gamma - e\gamma - (2p_0 q + q_u)/(1-q)\}$$
$$(e + fn_2) - \{c - e\gamma - f\gamma - (2p_0 - q_u)/(1+q)\}(d + en_2)]$$
$$A_3 = (d + en_2 - q'e - q'fn_1)\{b - d\gamma - e\gamma - (2p_0 q + q_u)/(1+q)\}$$
$$(e + fn_1) - \{c - e\gamma - f\gamma - (2p_0 - q_u)/(1+q)\}(d + en_1)$$
$$n_1 = \sqrt{d/f}, \qquad n_2 = -n_1$$
$$\gamma = (c-b)/(f-d), \qquad b = (k_2k_4 - k_1k_5)/(k_2 - k_5)$$
$$c = -(k_1 - k_4)/(k_2 - k_5), \qquad d = k_2k_5k_6/(k_2 - k_5)$$
$$e = k_2k_6/(k_2 - k_5), \qquad f = k_6(k_2 - k_5)$$
$$k_1 = \{1 + (\omega/E)\cdot(1-\nu^2)\}\, q_u$$
$$k_2 = q + (\omega/E)\{(1-\nu)q - \nu\}(1+\nu)$$
$$k_3 = -\omega$$
$$k_4 = \{1 + (k_6/E)\cdot(1+\nu)\nu\}\, q_u$$
$$k_5 = q + (k_6/E)\{\nu q - (1-\nu)\}(1+\nu)$$
$$k_6 = \omega/[q + (\omega/E)\{(1-\nu)q - \nu\}(1+\nu)]$$
$$q = \tan^2 \alpha \qquad \alpha = \pi/4 + \phi/2$$
$$q' = \tan^2 \alpha' \qquad \alpha' = \pi/4 + \phi'/2$$
$$q_u = 2c \tan \alpha$$

Here, the unknown parameter is S_1, namely the ratio R_1/R_2. R_1 is the radius of the elastic-softening boundary, and R_2 is the radius of the softening-flow boundary. We can obtain the solution for S_1 by an iterative numerical method on a hand-held calculator having several memory devices.

(3) To obtain the value of S_2.

$$S_2 = [\{c + e(\alpha + \beta - \gamma) + f(\alpha_1 n_1 + \beta_1 n_2 - \gamma) - q_u'/(1-q')\}/\{p_i - q_u/(1-q')\}]^{\frac{1}{q'-1}} \tag{19}$$

where

$$
\begin{aligned}
&S_2=R_2/a\\
&\alpha_1=(A_8-A_9)/A_{10}S_1^{n_1-1}\\
&A_8=\{b-d\gamma-e\gamma-(2p_0q+q_u)/(1+q)\}(e+fn_2)\\
&A_9=\{c-e\gamma-f\gamma-(2p_0-q_u)/(1+q)\}(d+en_2)\\
&A_{10}=(e^2-df)(n_2-n_1)\\
&\beta_1=(A_{11}-A_{12})/A_{13}S_1^{n_2-1}\\
&A_{11}=\{b-d\gamma-e\gamma-(2p_0q+q_u)/(1+q)\}(e+fn_1)\\
&A_{12}=\{c-e\gamma-f\gamma-(2p_0-q_u)/(1+q)\}(d+en_1)\\
&A_{13}=(e^2-df)(n_1-n_2)
\end{aligned}
$$

By this equation we can obtain the value of S_2. S_2 is the ratio of R_2/a. Here we can see the softening-flow boundary.

(4) To obtain the strains, stresses and displacement of the wall.

$$
\left.
\begin{aligned}
&\epsilon_t^*=(\alpha_1+\beta_1-\gamma)S_2/a, \qquad \epsilon_r^*=-\epsilon_t^*\\
&\sigma_t^*=q_u'/(1-q')+q'\{p_i-q_u'/(1-q')\}\\
&\sigma_r^*=q_u'/(1-q')+\{p_i-q_u'/(1-q')\}\\
&u^*=\{(\alpha_1+\beta_1-\gamma)-p_0/2(\lambda+\mu)\}S_2^2\cdot a\\
&\epsilon_p^*=\epsilon^*-\epsilon_e^*\\
&\epsilon^*=\epsilon_t^*-\epsilon_r^* \qquad \epsilon_e^*=(\sigma_t^*-\sigma_r^*)/2\mu
\end{aligned}
\right\} \tag{20}
$$

Also through a similar procedure, we can obtain solutions for the case of the induced softening only.

Case of induced 'softening' only

(1) Solve the following equation. (S_3: unknown)

$$B_1S_3^{n_1-1}+B_2S_3^{n_1-n_2}+B_3=0\rightarrow S_3 \tag{21}$$

where

$$
\begin{aligned}
&S_3=R_1/a\\
&B_1=\{c-(e+f)\gamma-p_i\}\{fd-e^2\}(n_1-n_2)\\
&B_2=[(d+en_1)\{c-e\gamma-f\gamma-(2p_0-q_u)/(1+q)\}\\
&\qquad -(e+fn_1)\{b-d\gamma-e\gamma-(2p_0q+q_u)/(1+q)\}](e+fn_2)\\
&B_3=[(e+fn_2)\{b-d\gamma-e\gamma-(2p_0q+q_u)/(1+q)\}\\
&\qquad -(d+en_2)\{c-e\gamma-f\gamma-(2p_0-q_u)/(1+q)\}](e+fn_1)
\end{aligned}
$$

(2) Obtain the strains, stresses and displacement of the wall.

$$\epsilon_t^*=\alpha_2+\beta_2-\gamma \qquad \epsilon_r^*=\alpha_2\cdot n_1+\beta_2\cdot n_2-\gamma \tag{22}$$

where

$$\alpha_2=\{(1-S_3^{n_2-1})(c-e\gamma-f\gamma)-(2p_0-q_u)/(1+q)+p_iS_3^{n_2-1}\}/\{(e+fn_1)(S_3^{n_2-1}-S_3^{n_1-1})\}$$
$$\beta_2=\{(1-S_3^{n_1-1})(c-e\gamma-f\gamma)-(2p_0-q_u)/(1+q)+p_iS_3^{n_1-1}\}/\{(e+fn_2)(S_3^{n_1-1}-S_3^{n_2-1})\}$$

$$\left.\begin{aligned}&\sigma_t^*=b+d\epsilon_t^*+e\epsilon_r^* \qquad \sigma_r^*=c+e\epsilon_t^*+f\epsilon_r^*\\&u^*=(\alpha_2+\beta_2-\gamma)a-p_0a/2(\lambda+\mu)\\&\epsilon_p^*=\epsilon^*-\epsilon_e^*\\&\epsilon^*=\epsilon_t^*-\epsilon_r^* \qquad \epsilon_e^*=(\sigma_t^*-\sigma_r^*)/2\mu\end{aligned}\right\} \tag{23}$$

6. Relation among Plastic Zone, Inner Pressure and Competence Factar

Here, let us go back to the discussion about the strain softening behavior.

Fig. 19 ((a), (b) and (c)) shows the results of a parametric study with respect to W_p, C_f and p_i under the same condition of $p_0=2\times10^3$ kN/m². It can be seen that a small change of p_i has a large influence on W_p. Also, a higher p_i makes W_p much less even in the case of $C_f=0.5$, equal to the average value for the Middle Sector. Namely, when such a poor support system as $p_i=200$ kN/m² was placed, the plasticized zone

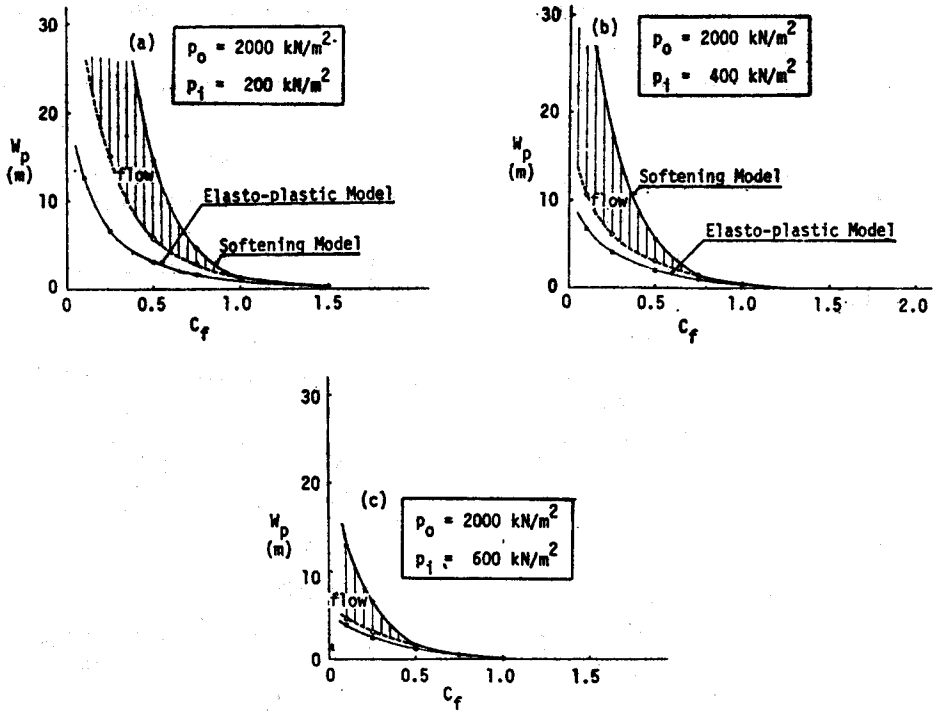

Fig. 19 Relations among W_p, C_f and p_i

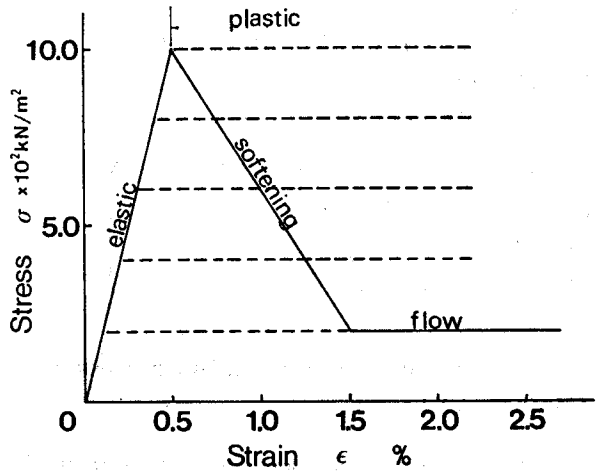

Fig. 20 Stress-strain relation for an elastic-plastic model

(W_p) exceeded 15 m for the case of $C_f=0.5$, and a fairly poor support system, giving only $p_i=400$ kN/m², resulted in a 7 m wide plastic zone. In Fig. 19, the results obtained by the elasto-plastic model with no consideration of the reduction of the peak strength are also plotted. When the support system gives $p_i=600$ kN/m², no flow zone is induced for the case of $C_f=0.5$, and the result obtained by the softening model agrees with that of the elasto-plastic model, as shown in Fig. 19 (c).

The comparison of the obtained results between the softening model and the elasto-

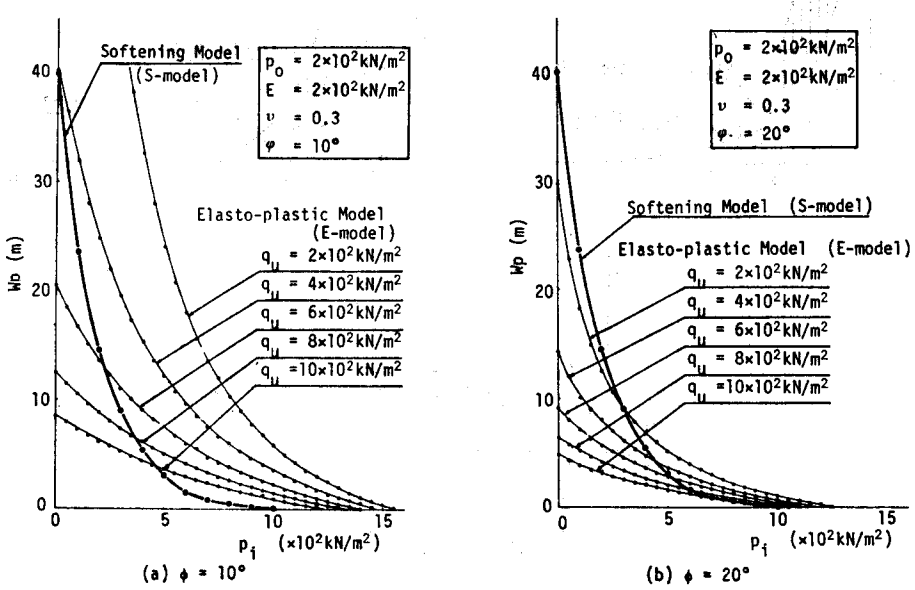

Fig. 21 Difference of W_p between an elasto-plastic and a strain softening

plastic model is interesting, since many people use an elasto-plastic model beacuse of its easy application. In order to get some results by an elasto-plastic model, it is required to establish some bi-linear stress-strain relations, which are expressed by the positive solid line and the dotted lines as shown in Fig. 20. By assuming $q_u=2$, 4, 6, 8 and 10×10^2 kN/m^2 for $p_0=2\times10^3$ kN/m^2, $E=2\times10^5$ kN/m^2, $\nu=0.3$, $\phi=20°$; $\phi=10°$, Eqs. (1), (2) and (3) give W_p, U_w and ε_p respectively. The results with respect to W_p are plotted by the thin curves shown in Fig. 21, in which (a) and (b) correspond to the cases of $\phi=10°$ and 20° respectively. Also, the results of the strain-softening model are plotted by the thick curves in (a) and (b), where the curves are the same because of considering $\phi=20°$ at peak and $\phi'=10°$ at the residual at the same time. As shown in these figures, there exists a big difference between these two types of models, and thus it is quite difficult to consider a strain softening phenomenon by a bi-linear elastoplastic model.

Being based on further parametric studies under the condition of $p_0=2\times10^3$ kN/m^2, $E=2\times10^5$ kN/m^2, $\nu=0.4$ E, $\phi=20$, $\phi'=\frac{1}{2}\phi$ and $q_u'=\frac{1}{5}q_u$, Fig. 22 concludes the condition for the appearence of a flow zone. This relates the stability of an opening for the most part, with the introduction of a competence factor (C_f) and a support intensity factor (p_i/p_0). For example, no flow zone appears in the region of $p_i\geqq0.2p_0$ for the case of $C_f=1.0$, and $p_i\geqq0.6p_0$ is required for the case of $C_f=0.5$. This shows that the opening becomes unstable considering the decrease of the half-dome action if the supports had not been placed very close to the face after mining. When this condition is included in the shaded area, the result obtained by the elasto-plastic model, which maintains its

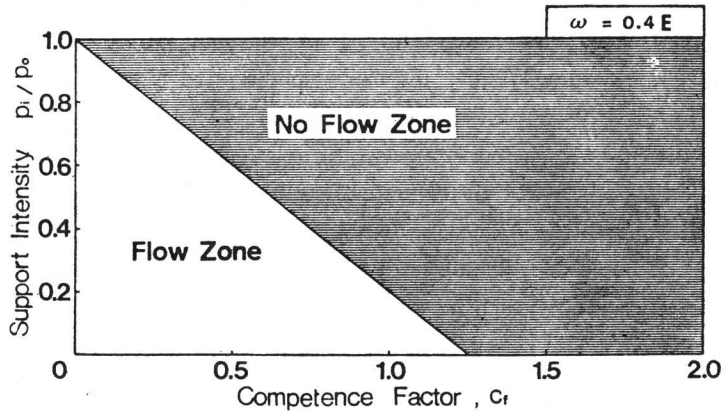

p_0: hydrostatic initial stress
q_u: unconfined compressive strength
E: elastic modulus
p_i: bearing force of supports
C_f: Competence factor
ω: negative slope of deformation coefficient in softening

Fig. 22 Condition for the appearence of flow zone

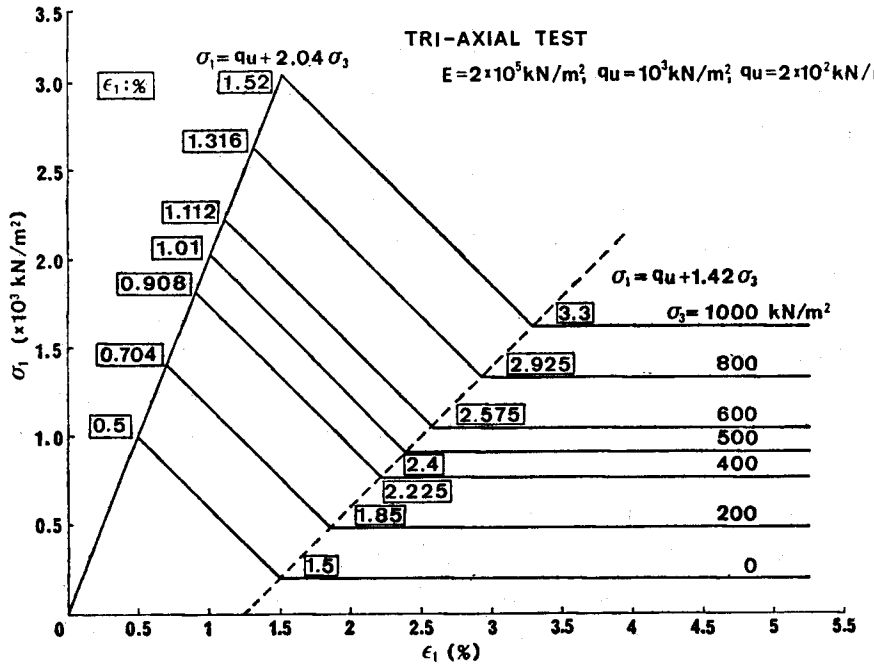

Fig. 23 Schematic stress-strain relation for tri-axial test

peak strength after yielding, will not show so serious a difference from the result by a strain softening model.

In order to get a better understanding of the strain softening model proposed by us, let us discuss the relation between the axial stress (σ_1) and the axial strain (ε_1) in the case of a tri-axial test. Also to be discussed will be the change of the stress in the simulation of the circular tunnel under the same condition of $C_f=0.5$ ($p_0=200$ kN/m², $q_u=1000$ kN/m², $E=2\times10^5$ kN/m², $\nu=0.3$, $\phi=20°$, $\phi'=10°$, $q_u'=200$ kN/m², $\omega=0.4E$). Fig. 23 shows a schematic stress-strain relation based on our assumption corresponding to a tri-axial test. In the state of strain softening, there exists the relation that the negative gradient of the deformation coefficient $-\omega(=-0.4E)$ is always unchanged. From the Mohr-Coulomb yield criteria, $\tau=C+\sigma\tan\phi$, the following equation is derived corresponding to each peak stress (σ_1) under a constant confining pressure (σ_3).

$$\sigma_1=q_u+2.04\sigma_3 \tag{24}$$

Also, the equation, $\tau=C'+\sigma\tan\phi'$ for the state of 'flow', gives another form as follows:

$$\sigma_1=q_u'+1.42\sigma_3 \tag{25}$$

Both Eq. (24) and Eq. (25) show a rather high increase of allowable stresses of σ_1 at the

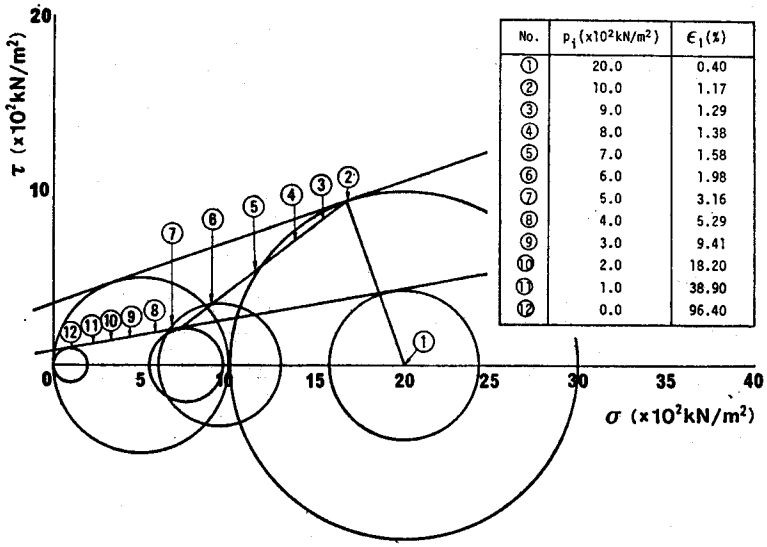

Fig. 24 The path of shear stresses associated with the advance of the face

peak and at the residual state, which are given by the increase of the confining pressure σ_3 at low levels, such as 100 to 500 kN/m². This fact might be important in explaining the effect of the supports acting on the tunnel wall as a sort of passive inner pressure, with the exception of the active pressure such as pre-stressed rockbolts, compressed air etc. In Fig. 23 the dotted line, corresponding to the boundary of the states between the softening and flow, expresses the increase of allowable axial strain associated with the confining pressure, which is a major proposition in our concept of designing supports.

In the case of a tunnel model, a Mohr circle expressing the initial state before excavation is a point at σ=2000 kN/m² (equal to p_0) and the shear stress τ becomes high, attendant upon the advance of the mining face until the circle touches the yielding line, $\tau=C+\sigma\tan\phi$ ($\tau=350+\sigma\tan 20°$ in kN/m²). Fig. 24 shows the path of shear stress caused by the advance of the face. From Point A, as the shear strength of the ground decreases gradually attendant upon strain softening, the shear stress follows the segment $\overline{AB}$, and 'flow' appears at Point B with ε_t=2.81%. After passing Point B, the increasing rate of the tangential normal strain ε_t (corresponding to ε_1 in the tri-axial test) becomes very high, and the magnitude of ε_t reaches 96.4% in the case of no support (equal to $p_i=0$). It can be estimated easily from this history of shear stress that the supports would be subjected to a large deformation and heavy load if the high normal strain ε_t was allowed beyond the state of Point B. Consequently, the maximum allowable strain should be designated by the magnitude not reaching the state of flow.

The stress state around the circular opening under the hydro-static initial stress field in the case of $p_0=2\times10^3$ kN/m², $q_u=10^3$ kN/m², $C_f=0.5$ is illustrated by Fig. 25.

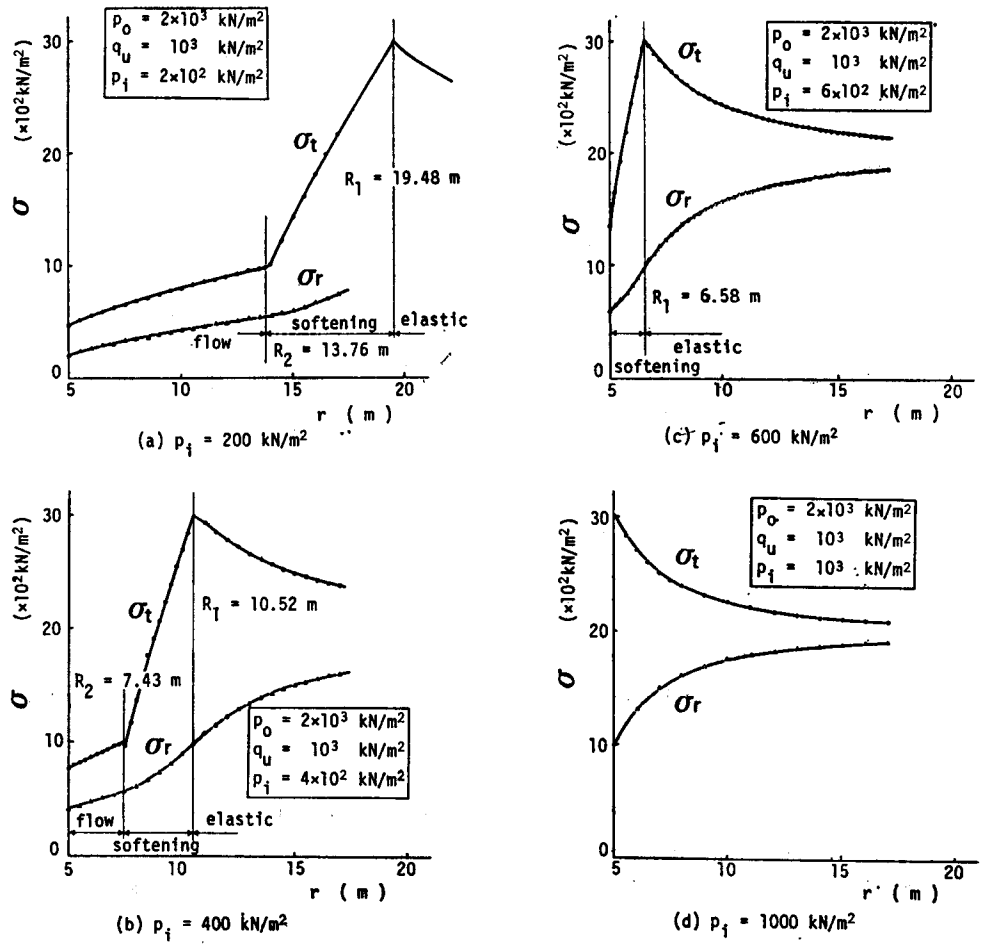

Fig. 25 Stress distribution around a circular opening in elastic, strain softening and flow state

The small increment of an inner pressure (p_i) such as 200 kN/m², which is equal to 10% of the initial stress (p_0) or of the final excavation force (p_e), changes the stress distribution in quite a different manner. Fig. 25 (a) shows the state in which the flow progresses, (b) shows the beginning of 'flow' ,(c) is the state in which no flow is induced and the stress reduction near the wall is intensive, and (d) is still in the elastic state under the load of p_i=10³ kN/m², 50% of p_0.

7. A Procedure of Designing Supports

To briefly explain the procedure for designing the support system, the significant steps are

(1) Determine the maximum allowable strain to be caused around an opening at the

final state, being based on laboratory tests such as tri-axial test, stiff loading test, direct shear test etc. and, if possible, some preliminary field measurements. Empirical data and engineering judgement should be considered.

(2) Analyze the softening behavior of the rock mass in case of $C_f \leqq 4$. The width of the plastic zone, maximum strain, plastic strain, stresses and displacement of the wall corresponding to the various magnitudes of the inner pressure to be given by the support system as a whole can be obtained by Eq. (18)–Eq. (23). Before calculation, 10 pieces of input data should be prepared. These are: radius of an opening (a), Young's modulus (E), Poisson's ratio (ν), unconfined compressive strength (q_u), angle of internal friction at peak strength (ϕ), negative gradient of deformation coefficient (ω), primary stress field (p_0), unconfined compressive strength at residual state (q_u'), angle of internal friction at residual strength (ϕ') and inner pressure (p_i).

(3) Set up magnitude of the inner pressure to be given by supports other than rockbolt support, being based on the results obtained by the softening analysis mentioned in Item (2). Also, depending on the stiffness of the supports and physical properties of the rock, the limit of the allowable displacement of the wall should be determined. Further, magnitude of the inner pressure given by the shotcrete lining ($(p_i)_{sc}$) and that given by the steel ribs ($(p_i)_{sr}$) would be set respectively with regard to the same magnitude of displacement. In this paper, no support other than rockbolting is mentioned in detail. However, it is a common and a fundamental concept of designing that so long as it is possible to replace the supporting effect by the equivalent inner pressure, every kind of support should be estimated with the consideration of a rapidly decreasing half-dome action from the face position. The procedure of designing itself mentioned in this item is easier than the following one with respect to rockbolts.

(4) Evaluate the magnitude of the inner pressure to be given by fully bonded rockbolt support, $(p_i)_{rb}$ at the confining level which can be set up in item (3).

(5) Monitor convergence, displacement of rock and stress increment in lining as major measurements for checking the stability of an opening and compatibility of the original design. The magnitude of the displacement of the wall (U_w) is most convenient and reliable as the monitored parameter. Being different from the preliminary field measurement executed before the construction, the monitoring system during construction should be as simple as possible from the point of view of time and handling.

(6) Estimate the magnitude of the supplementary supports (Δp_i) to be added, being based on the result obtained in the daily monitoring. Judging from the necessary magnitude of Δp_i and the convenience of the application of the basic construction procedure, some combinations among the following methods will be adapted:

setting rockbolts at increased density: spiling rockbolts for pre-reinforcement; face stabilization by rockbolts made of steel, fiberglass or high polymer resin which is placed perpendicularly to the face; secondary shotcrete lining with reinforcement mesh, fiber mixture, Bernold sheet etc.; placing supplementary steel ribs; grouting compressed air; segmented lining, with or without shield driving and so on.

From now, let us discuss the supports—ground interaction on the assumption that the competence factor is 0.5 (as a mean value) in the case of a circular tunnel with 10 m diameter. The inner pressure of 4 or 5×10^2 kN/m^2 is given by shotcrete lining and steel ribs, $((p_i)_1=(p_i)_{sc}+(p_i)_{sr})$, and a fully bonded rockbolt system gives some additional inner pressure, $(p_i)_{rb}$, being associated with the stress increment, Δp_e, caused by the advance of the face. Consequently, the wall is subjected to a total inner pressure, $(p_i)_1=(p_i)_{sc}+(p_i)_{rb}$, at the final state in which the tunnel should be stabilized as a ring structure.

Fig. 26 shows (a) W_p, (b) U_w, (c)ε_1* and (d) the change of p_i given by the face as well as the excavation force p_e, having the relation $[p_i+p_e=p_0=2\times10^3$ kN/m$^2]$, on the same abscissa expressing the manitude of p_i. In order to distinguish p_i given by the half-dome action from other artificial supports, let us denote $(p_i)_f$ as

$$(p_i)_f+p_e=p_0=2\times10^3 \text{ kN/m}^2 \tag{26}$$

$(p_i)_f$, which is equal to $p_0=2000$ kN/m^2 initially, begins to decrease at $d=-15$ m ahead

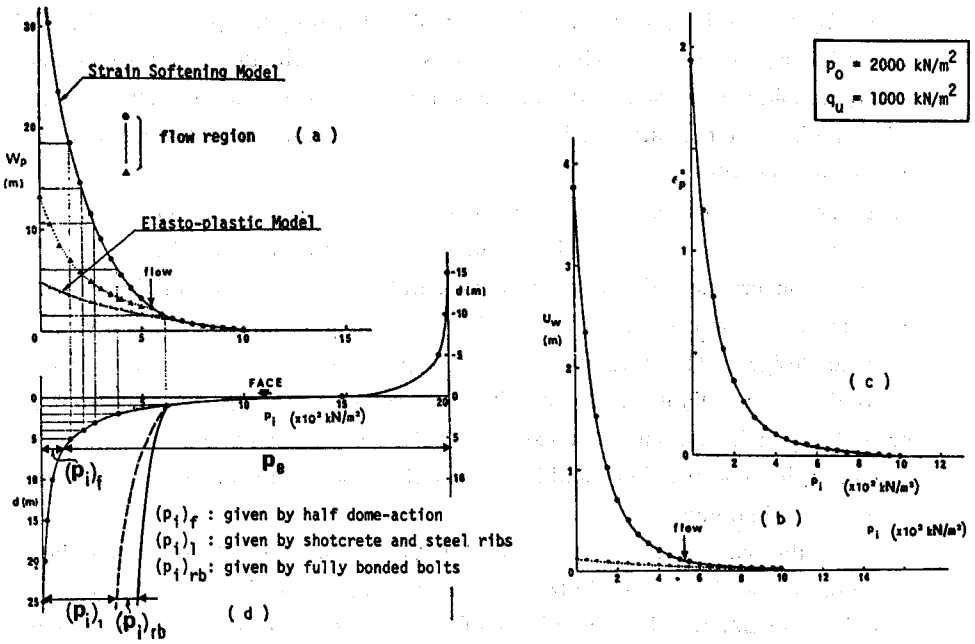

Fig. 26 Decrease of half-dome action and relations among W_p, U_w, ε_p* and p_i in case of $C_f=0.5$

of the face. It becomes approximately 1.5×10^3 kN/m^2 at the face position and diminishes at the section about d=25 m behind the face. Within 1 m behind the face, $(p_i)_f$ decreases from 1.5×10^3 kN/m^2 to 600 kN/m^2 (corresponding to 'from d=0 to d=1 m'). This means that the face loses 45% of its original bearing capacity as a temporary support only 1 m behind the face. This is considered one of the main reasons why such concrete operations as placing rockbolts and shotcrete lining to the face position as early and close as possible are required in the application of the New Austrian Tunnelling Method (NATM). When the face advances one more meter, namely from d=1 m to 2 m, $(p_i)_f$ varies from 6 to 4×10^2 kN/m^2. Being associated with this 1 m advance, the width of the plastic zone (W_p) develops from 1.6 m to 5.5 m according to Fig. 26 (a). At the position of d=0 m, no plastic zone occurs and the width of the plastic ring (W_p), softening ring (W_1) and flow ring (W_2) at each position behind the face are as follows.

at d=0 m:	W_p=0 m	W_1=0 m,	
at d=1 m:	W_p=1.58 m,	W_1=1.58 m,	W_2=0 m
at d=1.25 m:	W_p=3.13 m,	W_1=2.39 m,	W_2=0.74 m
at d=2 m:	W_p=5.52 m.	W_1=3.09 m,	W_2=2.42 m
at d=5 m:	W_p=18.39 m,	W_1=6.89 m,	W_2=11.52 m
at d=10 m:	W_p=30.40 m,	W_1=10.40 m,	W_2=20.00 m
at d=25 m:	W_p=39.90 m,	W_1=13.19 m,	W_2=26.72 m

where, notations are subject to Fig. 17 and the relation, $W_p=W_1+W_2$, is realized.

8. Conclusion

Concerning tunnel driving and rockbolting in rock which shows a strain softening behavior, the following may be concluded.

1) The mining face plays an important role as a temporary support, due to half-dome action, and when advancing the face, it is necessary to place artificial supports, as a substitute for the half-dome action, within a span length from the face, so as to mobilize the bearing capacity of the rock mass as fully as possible.

2) As the effects of the systematic supports are the mobilizing of confining stress and the decreasing of shear stress, a procedure to design supports can be proposed, based on the idea of replacing the effects of supports by an inner pressure acting on the surface of the tunnel wall. By employing this inner pressure as the main parameter, it is possible to calculate the width of the plastic zone, the displacement of the wall and the plastic strain near the wall.

3) The half-dome action of the face is formed within a range of double the length of the span or the height, in the vicinity of the face.

4) Convergence survey means monitoring the change of the radial-normal stress or extraction force, as well as the displacement of the wall.

5) Concerning a tunnel in rock whose competence factor is less than 1.0, it is difficult to evaluate the plastic zone without consideration of the strain softening behavior. The equations presented in this paper give solutions for stresses, strains and displacements in the case of a circular opening.

Acknowledgement

Grateful acknowledgements are made to Drs. L. Müller, H. Habenicht and G. Sauer in Salzburg; Prof. R. Goodman, University of California; Prof. E. Cording, University of Illinois; Dr. P. Egger, Lausanne Polytechnic; Prof. S. Kobayashi and Associate Prof. N. Adachi, Kyoto Univerity; Messrs. K. Hama, A. Yokoyama and M. Ohtuka, Japan Railway Construction Authority for their stimulating discussions and constructive criticisms. Messrs. K. Kimura, A. Nishihara and K. Kaiya, graduate students of Kyoto University, are also thanked for their help in the calculations and drawings.

References

1) Muirwood, A.: Tunnels for roads and motorways, The quarterly J. of Engineering Geology, Vol. 5, No. 1 & 2, pp. 119–120, 1972.
2) R. Nakano: Geotechnical properties of mudstone of Neogene tertiary in Japan, Proc. Int'l Sympo. on Soil Mechanics, Oaxaca, Mexico, Vol. 1, pp. 75–92, 1979.
3) S. Hata, C. Tanimoto, K. Kimura: Field measurement and consideration of deformability of the Izumi Layers, Rock Mechanics, Suppl. 8, pp. 349–367, 1979.
4) Report on the investigation of the earth/rock pressure in Seikan Tunnel, JSCE, pp. 352, 1977. (in Japanese)
5) S. Hata, C. Tanimoto: Deformation of Nabetachiyama Tunnel and expansive behavior of mudstone, Technical report for Japan Railway Construction Authority, March 1979. (in Japanese)
6) S. Hata, C. Tanimoto, K. Kimura: Evaluation of rockbolt effect in tunnelling, 12th Sympo. on Rock Mechanics, pp. 61–65, JSCE, 1979. (in Japanese)
7) T. Inoue, T. Kawahara, S. Miyabayashi: Challenge to tunnelling through expansive mudstone—Nabetachiyama Tunnel, Tunnels and Underground, Vol. 9, No. 4, pp. 7–14, April 1978. (in Japanese)
8) K. Sugawara, C. Tanimoto: Strain softening behavior around a circular opening—Analytical solution, Int. J. of Rock Mechanics and Mining Science (under submitting).